ICAS Paper No. 70-26

SOME PROBLEMS OF AIRCRAFT CONTROL SURFACES AERODYNAMICS

by
V. G. Mikeladze
Chief, Aerodynamics Laboratory
Central Aero-Hydrodynamic Institute
Moscow, USSR

The Seventh Congress of the International Council of the Aeronautical Sciences

CONSIGLIO NAZIONALE DELLE RICERCHE, ROMA, ITALY / SEPTEMBER 14-18, 1970

Price: 400 Lire

SOME PROBLEMS OF AIRCRAFT CONTROL SURFACES AERODYNAMICS

V.G. Mikeladze
Chief, Aerodynamic Laboratory Central Aerodynamic Institute
Radio str. 17 Moscow USSR

Aerodynamic characteristics of low-aspect-ratio wing elevons with variable-sweep leading edge as longitudinal and lateral controls are considered.

An estimation method of elevon aerodynamic characteristics with the use of the reversibility theorem at subsonics and the linear theorem at supersonics is presented; a physical pattern of flow past a low-aspect-ratio wing with elevons extended to high angles by means of pressure distribution at subsonic, transonic and supersonic speeds is shown.

The results of systimatic analitical and experimental investigations of particular elevon parameters effect on their aerodynamic characteristics are given.

I. A Method of Estimating Elevon Effectiveness for Arbitrary Plan-Form Wings at Subsonic Speeds

A method of estimating elevons effectiveness for arbitrary plan-form wings at subsonic speeds is based on the use of the reversibility theorem, which relates aerodynamic characteristics of a wing in direct and reverse flow when the velocity direction of free flow V_0 is reversed.

The values of the derivatives of the lift coefficient $C_{L\delta e}$, pitching moment coefficient $C_{m\delta e}$ and rolling moment coefficient $C_{l\delta e}$ with respect to the elevon deflection angle δe can be written as

$$C_{L\delta e} = \frac{1}{S}\iint_{S_e} \bar{P}_{\alpha-}\, ds \qquad (1)$$

$$C_{m_1\delta e} = \frac{1}{S}\iint_{S_e} \bar{P}_{\omega z-}\, ds \qquad (2)$$

$$C_{l_1\delta e} = \frac{1}{S}\iint_{S_e} \bar{P}_{\omega x-}\, ds \qquad (3)$$

where $C_{m_1\delta e}$ and $C_{l_1\delta e}$ are the pitching moment coefficient and rolling moment coefficient for which the wing root chord C_0 is taken as a characteristic linear dimension

$\bar{P}_{\alpha-} = \frac{\Delta P_\alpha}{q}$ - pressure differential coefficient between the lower and upper surfaces of the wing in reverse flow when the wing at the angle of attack moves without rotation

$\bar{P}_{\omega z-} = \frac{\Delta P_{\omega z}}{q}$ - pressure differential coefficient in reverse flow when the wing rotates about OZ axis

$\bar{P}_{\omega x-} = \frac{\Delta P_{\omega x}}{q}$ - pressure differential coefficient in reverse flow when the wing rotates about OX axis

$q = \frac{\rho V_0^2}{2}$ - dynamic pressure

The expressions 1 to 3 show that it is sufficient to define the values of $\bar{P}_{\alpha-}$, $\bar{P}_{\omega z-}$ and $\bar{P}_{\omega x-}$ for a wing in reverse flow, then the coefficients $C_{L\delta e}$, $C_{m\delta e}$ and $C_{l\delta e}$ may be found by simple integration. The problem of flow past a wing in reverse flow is solved by a method in which the wing is substituted by a vortex surface. The lifting vortex surface is simulated by a number of bound vortex cords. Each vortex cord is substituted by several skew horseshoe vortices. Each skew horseshoe vortex consists of a bound vortex of constant strength along the span Γ_i and free vortices. The design scheme of the wing is shown in fig. 1.

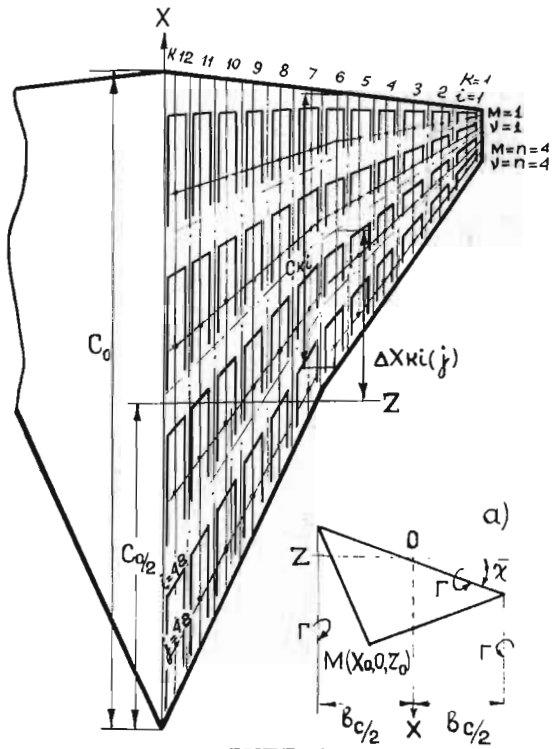

FIGURE I.

For the given case of elevon effectiveness estimation the wing with a cranked leading edge was substituted by four vortex cords along the chord and each of the latter was substituted by twelve

skew horseshoe vortices along the half-wing span.

Thus on the starboard wing there are forty-eight bound vortices and on the port wing the same number of bound vortices. In each mesh of the net obtained a bound vortex coincides with a quarter-chord line of the mesh and the distance between free vortex cords is equal to the mesh span. Constraint boundary conditions are satisfied for each mesh at the mid-point of a three-quarter-chord line.

In estimating elevon effectiveness it is necessary to know the values of a vortex dimensionless circulation: for a wing at the angle of attack moving without rotation $\gamma_{\alpha i}$, for a wing rotating about the axis OZ $\gamma_{\omega z i}$ and for a wing rotating about the axis OX $\gamma_{\omega x i}$.

When boundary conditions were satisfied three independent sets of equations were obtained which allowed three previously mentioned dimensionless circulations to be determined

$$\left.\begin{aligned}
&\sum_{i=1}^{m}(W_{yij}+\Delta W_{yij})\gamma_{\alpha i}=-2\pi\\
&\sum_{i=1}^{m}(W_{yij}+\Delta W_{yij})\gamma_{\omega z i}=2\pi\frac{x_{oj}}{C_o}\\
&\sum_{i=1}^{m}(W_{yij}-\Delta W_{yij})\gamma_{\omega x i}=-2\pi\frac{z_{oj}}{C_o}
\end{aligned}\right\}\ j=1,2\ldots m \qquad m=N\cdot n \qquad (4)$$

where $W_{yij}=W_y(\xi_{oij},\zeta_{oij},\chi)$ are dimensionless velocities, due to a skew horseshoe vortex i at the point j; $\Delta W_{yij}=W_y(\xi_{oij},\Delta\zeta_{oij},\chi)$ are additional dimensionless velocities which arise at the point j due to a vortex on the port wing and a symmetrical vortex i. The calculation of all dimensionless velocities was made according to the following formulae

$$W_y=\frac{V_{oj}}{2\pi}W_y(\xi_o,\zeta_o,\chi) \qquad (5)$$

where

$$W_y(\xi_o,\zeta_o,\chi)=U_y(\xi_o,\zeta_o,\chi)+V_y(\xi_o,\zeta_o,\chi) \qquad (6)$$

Here

$\gamma=\frac{\Gamma}{V_o l_c}$ - dimensionless circulation of a vortex

l_c - distance between free vortices (see fig.1)

$\xi_o=\frac{x_o}{l_c/2};\ \zeta_o=\frac{z_o}{l_c/2}$ - dimensionless coordinates at the point M

χ - bound vortex sweep angle

$U_y(\xi_o,\zeta_o,\chi)$ - velocity due to a bound vortex at an arbitrary point

$V_y(\xi_o,\zeta_o,\chi)$ - velocity due to free vortices at an arbitrary point

$$U_y(\xi_o,\zeta_o,\chi)=\frac{1}{\xi_o\cos\chi+\zeta_o\sin\chi}\times$$

$$\times\left[\frac{\xi_o\sin\chi-\zeta_o\cos\chi+\frac{1}{\cos\chi}}{\sqrt{(\xi_o+tg\chi)^2+(1-\zeta_o)^2}}+\right.$$

$$\left.+\frac{\frac{1}{\cos\chi}-\xi_o\sin\chi+\zeta_o\cos\chi}{\sqrt{(\xi_o-tg\chi)^2+(1+\zeta_o)^2}}\right] \qquad (7)$$

$$V_y(\xi_o,\zeta_o,\chi)=\frac{1}{1-\zeta_o}\left[1+\frac{\xi_o+tg\chi}{\sqrt{(\xi_o+tg\chi)^2+(1-\zeta_o)^2}}\right]-$$

$$-\frac{1}{1-\zeta_o}\left[1+\frac{\xi_o-tg\chi}{\sqrt{(\xi_o-tg\chi)^2+(1+\zeta_o)^2}}\right] \qquad (8)$$

After solving the set of equations (4) and estimating the values $\bar{P}_{\alpha-}$, $\bar{P}_{\omega z-}$ and $\bar{P}_{\omega x-}$ we find total characteristics of the wing with deflected elevons according to the following formulae:

$$C_{L\delta e}=\lambda\int_{\bar{z}_1}^{\bar{z}_2}\psi_{\gamma\alpha}\,d\bar{z} \qquad (9)$$

$$C_{m_z\delta e}=\lambda\int_{\bar{z}_1}^{\bar{z}_2}\psi_{\gamma\omega z}\,d\bar{z} \qquad (10)$$

$$C_{l_x\delta e}=\lambda\int_{\bar{z}_1}^{\bar{z}_2}\psi_{\gamma\omega x}\,d\bar{z} \qquad (11)$$

where $\lambda=\frac{l^2}{S}$ is wing aspect ratio

$$\psi_{\gamma\alpha}=\frac{1}{2\cdot57{,}3}\int_{\bar{x}^*-\bar{c}_e}^{\bar{x}^*}\bar{P}_{\alpha-}\,d\bar{x} \qquad (12)$$

$$\psi_{\gamma\omega_z} = \frac{1}{2\cdot 57{,}3}\int_{\bar{x}^*-\bar{c}_e}^{\bar{x}^*} \bar{p}\omega_z \, d\bar{x} \qquad (13)$$

$$\psi_{\gamma\omega_x} = \frac{1}{2\cdot 57{,}3}\int_{\bar{x}^*-\bar{c}_e}^{\bar{x}^*} \bar{p}\omega_x \, d\bar{x} \qquad (14)$$

Here x^* - coordinate of the wing section leading edge in reverse flow

$\bar{c}_e$ - elevon chord ratio

Parametric computations of elevon effectiveness were made by using high-speed electronic computers. As an example the results of elevon effectiveness calculations for the wing with a cranked leading edge are shown in figs 2 to 4.

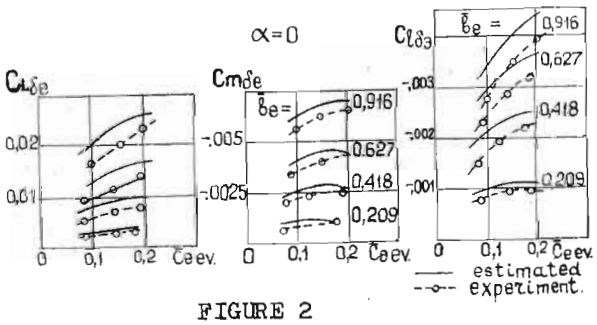

FIGURE 2

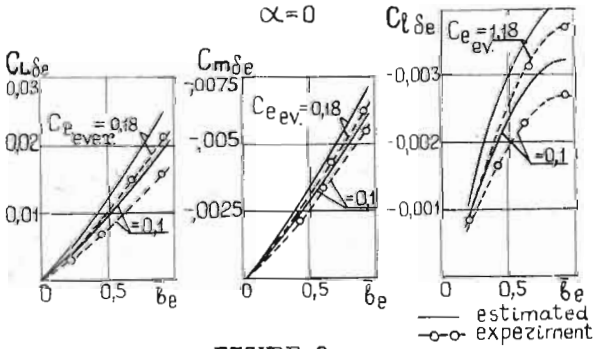

FIGURE 3

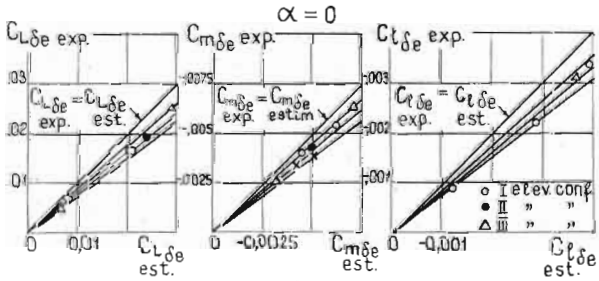

FIGURE 4

The effect on elevon effectiveness of elevon geometric parameters - aspect ratio and chord ratio - is shown. The correlation of theoretical results and experimental data in terms of the derivatives $C_{L\delta e}$, $C_{m\delta e}$ and $C_{l\delta e}$ shows that the predicted values of the coefficients $C_{L\delta e}$, $C_{m\delta e}$ and $C_{l\delta e}$ exceed the test data. One of the reasons of such discrepancy is the presence of gaps (which are not taken into accont in the theory) occuring between the fixed part of the wing and the deflected elevon. The effect of the gap on elevon effectiveness is shown in fig. 5.

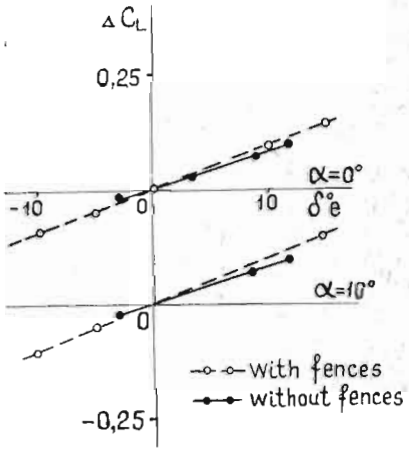

FIGURE 5

The inclusion of empirical coefficients into the predicted values of the derivatives $C_{L\delta e}$, $C_{m\delta e}$ and $C_{l\delta e}$ enables to obtain these derivatives with an accuracy ± 5%.

II. A Method for Estimating Elevon Effectiveness and Hinge-Moments at Supersonic Speeds

a. The effectiveness of elevons.

The estimation method of the effectiveness of the elevons for low-aspect-ratio wings at supersonic speeds is based on the linearized theory for supersonic flow. When estimating the elevon effectiveness it is assumed that the elevon hinge line is supersonic, the Mach lines do not intersect the wing and elevon chords. The elevon with adjacent parts of the wing is divided into regions (fig. 6):

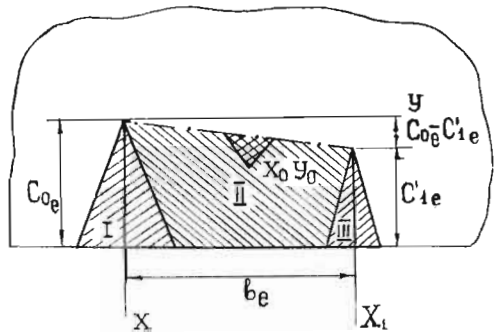

FIGURE 6

Region I is bounded by the Mach lines from the point of intersection of the hinge line with the elevon root chord and trailing edge.

Region II is bounded by the Mach lines from the point of intersection of the hinge line with the elevon root and tip chords, the elevons hinge line and trailing edge.

Region III is bounded by the Mach lines from the point of intersection of the hinge line with the elevon tip chord and trailing edge.

In these regions the pressure differential coefficient is

$$\bar{p}_{I\delta e}=\frac{4}{\pi\sqrt{\beta^2-tg^2\chi_e}}\arccos\frac{\alpha-\beta\,y/x}{1-\alpha\beta\,y/x} \tag{15}$$

$$\bar{p}_{II\delta e}=\frac{4}{\sqrt{\beta^2-tg^2\chi_e}} \tag{16}$$

$$\bar{p}_{III\delta e}=\frac{4}{\pi\sqrt{\beta^2-tg^2\chi_e}}\arccos\frac{\beta\,y/x-\alpha}{1-\alpha\beta\,y/x} \tag{17}$$

In this formulae:

$\bar{p}_{i\delta}$ - is the pressure coefficient difference between the upper and lower elevon surfaces in the i-th region when the elevon deflected by 1 radian $\alpha=\frac{tg\chi_e}{\beta}$, where χ_e is the elevon hinge line sweep

$\beta=\sqrt{M^2-1}$

δe - is the elevon deflection determined at a streamwise section

For the low-aspect-ratio wings including the wing with the variable-sweep leading edge and the trailing edge normal to an axis of symmetry, the expressions for the derivatives $C_{L\delta e}$, $C_{m\delta e}$ and $C_{l\delta e}$, which characterize the effectiveness of elevons as the longitudinal and lateral stability controls, will be

$$C_{L\delta e}=\frac{4S_\Delta tg\varepsilon}{57{,}3S\sqrt{\beta^2-tg^2\chi_e}}\left[\frac{(\bar{C}_{0e}^2-\bar{C}_{1e}^2)(\sqrt{1-a^2}-1)}{tg\chi_e}+\right.$$

$$\left.+(\bar{C}_{0e}+\bar{C}_{1e})\bar{b}_e\right] \tag{18}$$

$$C_{l\delta e}=-\frac{2S_\Delta b_\Delta tg\varepsilon}{57{,}3Sb\sqrt{\beta^2-tg^2\chi_e}}\left\{\frac{\sqrt{1-a^2}-1}{tg\varepsilon}\times\right.$$

$$\times\left[(\bar{C}_{0e}^2-\bar{C}_{1e}^2)\bar{Z}_{0e}-\bar{C}_{1e}^2\bar{b}_e+\frac{\bar{C}_{0e}^3-\bar{C}_{1e}^3}{3tg\chi_e}\right]+$$

$$\left.+(\bar{C}_{0e}+\bar{C}_{1e})\bar{C}_e\,\bar{Z}_{0e}+\frac{1}{3}(\bar{C}_{0e}+2\bar{C}_{1e})\bar{C}_e^2\right\} \tag{19}$$

$$C_{m\delta e}=-\frac{1}{57{,}3}\left[C_{mI\delta e}+C_{mII\delta e}+\right.$$

$$\left.+C_{mIII\delta e}+C_{LIII\delta e}(\bar{C}_{0e}-\bar{C}_{1e})\frac{b_\Delta/2}{C_A}\right] \tag{20}$$

where

$$C_{mI\delta e}=\frac{8}{3}\,\frac{C_{0\Delta}S_\Delta tg^2\varepsilon(a-1+\sqrt{1-a^2})\bar{C}_{0e}^3}{C_A S tg\chi_e\sqrt{\beta^2-tg^2\chi_e}} \tag{21}$$

$$C_{mII\delta e}=\frac{4}{3}\,\frac{C_{0\Delta}S_\Delta tg^2\varepsilon}{C_A S\beta\sqrt{\beta^2-tg^2\chi_e}}\left[3\beta\bar{C}_e\bar{C}_{0e}^2-\right.$$

$$\left.-(\bar{C}_{0e}-\bar{C}_{1e})^2\beta\bar{b}_e-(\bar{C}_{0e}-\bar{C}_{1e})^3-\bar{C}_{0e}^2(\bar{C}_{0e}+3\bar{C}_{1e}^3)\right] \tag{22}$$

$$C_{m_{III}\delta e} = \frac{8}{3}\,\frac{C_{0\Delta} S_\Delta tg^2\varepsilon (a-1+\sqrt{1-a^2})\,\bar{C}_{1e}^3}{C_A S tg\chi_e \sqrt{\beta^2 - tg^2\chi_e}} \qquad (23)$$

$$C_{L_{III}\delta e} = \frac{4 S_\Delta \bar{C}_{1e}^2 tg\varepsilon}{S tg\chi_e \sqrt{\beta^2 - tg^2\chi_e}}\,(1+a-\sqrt{1-a^2}) \qquad (24)$$

In these formulae:

$C_{L\delta e}$ - lift coefficient due to both elevons deflection in the same direction by 1 deg

$C_{l\delta e}$ - rolling-moment coefficient due to both elevons deflection in opposite directions by ± 1 deg

$C_{m\delta e}$ - pitching-moment coefficient about Z - axis, passing the intersection of the elevon root chord with the elevon hinge line (fig. 7) when both elevons deflected in the same direction by 1 deg

$S_\Delta, C_{0\Delta}, b_\Delta$ ε - area, root chord, span and semiapex angle of the basic delta wing respectively (fig. 7)

$\bar{C}_{0e} = \frac{C_{0e}}{b_\Delta/2}; \bar{C}_{1e} = \frac{C_{1e}}{b_\Delta/2}; \bar{Z}_{0e} = \frac{Z_{0e}}{b_\Delta/2}$ - chord ratio, span and the root chord coordinate based to the basic-delta wing half-span

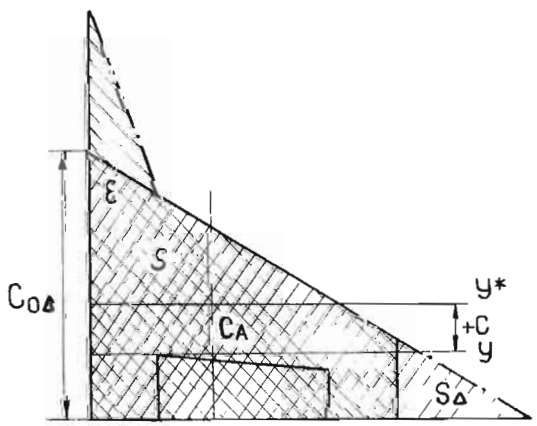

FIGURE 7

Recalculation of the pitching-moment coefficient to any center-of-gravity positions is made from the formula

$$C^*_{m\delta e} = C_{m\delta e} - C_{L\delta e}\,\bar{d} \qquad (25)$$

where $C_{L\delta e}$ is determined from the formule (18)

$\bar{d} = \frac{d}{C_A}$ - relative distance between axes, positive when Z* axis is ahead of Z - axis

In the case of the elevon constant absolute chord ($\chi_e = 0$) the expression for the derivatives $C_{L\delta e}$, $C_{l\delta e}$ and $C_{m\delta e}$ will be significantly simplified:

$$C_{L\delta e} = \frac{8 S_\Delta \bar{C}_e \bar{b}_e tg\varepsilon}{57{,}3\, S\beta} \qquad (26)$$

$$C_{l\delta e} = -\frac{2 S_\Delta b_\Delta \bar{C}_e \bar{b}_e tg\varepsilon}{57{,}3\, S b\beta}\,(2\bar{Z}_{0e} + \bar{b}_e) \qquad (27)$$

$$C_{m\delta e} = -\frac{4 S_\Delta C_{0\Delta} tg^2\varepsilon \bar{b}_e \bar{C}_e^2}{57{,}3\, S\, C_A \beta} \qquad (28)$$

The calculated characteristics of ele - vons effectiveness are higher than the experimental ones.

The experimental data reduction and comparison with the calculated results show that for the elevon effectiveness estimation at moderate supersonic speeds the values of the derivatives $C_{L\delta e}$, $C_{l\delta e}$, $C_{m\delta e}$ which were determined from the formulae (18), (19), (20), must be multiplied by the empirical coefficient $K_э = 0{,}85 \div 0{,}9$.

b. The elevon hinge-moments.

The elevon hinge-moments are calculated with using the same limitations as in the elevon effectiveness calculation. The hinge-moment coefficient about the hinge-line of the elevon, deflected by 1 deg, equals

$$C_{he} = -\frac{1}{57{,}3}\,(C_{he_I} + C_{he_{II}} + C_{he_{III}}) \qquad (29)$$

where

$$C_{he\,I} = \frac{8\bar{C}_{0e}^3 \operatorname{tg}\varepsilon}{3\bar{S}_e \bar{C}_{Ae} \operatorname{tg}\chi_e \sqrt{\beta^2 - \operatorname{tg}^2\chi_e}} \left\{ \alpha - 1 + \right.$$

$$\left. + \frac{\sqrt{1-\alpha^2}}{2}\left(\frac{1}{2} - \frac{\alpha}{\pi}\right) + \frac{\arccos\alpha}{2\pi} + \frac{1-\alpha^2}{2} \right\} \quad (30)$$

$$C_{he\,II} = \frac{4\operatorname{tg}\varepsilon}{\bar{S}_e \bar{C}_{Ae} \beta \sqrt{\beta^2 - \operatorname{tg}^2\chi_e}} \left[\left[\frac{1}{3} \left\{ \bar{C}_{0e}^2 \left[3\bar{b}_e\beta - \right.\right.\right.$$

$$\left. - 4\bar{C}_{0e} + 3(\bar{C}_{0e} - \bar{C}_{1e}) \right] - (\bar{C}_{0e} - \bar{C}_{1e})^2 \left[\bar{b}_e\beta + \right.$$

$$\left. + (\bar{C}_{0e} - \bar{C}_{1e}) \right] \Big\} - \operatorname{tg}\chi_e \left\{ \bar{b}_e \bar{C}_{0e} \left[\bar{b}_e\beta - \bar{C}_{0e} + 2(\bar{C}_{0e} - \bar{C}_{1e}) \right] - \right.$$

$$- \bar{b}_e (\bar{C}_{0e} - \bar{C}_{1e}) \left[\frac{2}{3}\bar{b}_e\beta + (\bar{C}_{0e} - \bar{C}_{1e}) \right] -$$

$$\left. \left. - \frac{\bar{C}_{0e}\bar{C}_{1e}(\bar{C}_{0e} - \bar{C}_{1e})}{\beta} - \frac{(\bar{C}_{0e} - \bar{C}_{1e})^2}{\beta} \right\} \right] \quad (31)$$

$$C_{he\,III} = \frac{8\bar{C}_{1e}^3 \operatorname{tg}\varepsilon}{3\bar{S}_e \bar{C}_{Ae} \operatorname{tg}\chi_e \sqrt{\beta^2 - \operatorname{tg}^2\chi_e}} \left\{ \alpha + \right.$$

$$\left. + \frac{\sqrt{1-\alpha^2}}{2}\left(\frac{1}{2} - \frac{\alpha}{\pi}\right) + \frac{\arccos\alpha}{2\pi} - \frac{1-\alpha^2}{2} \right\}$$

(32)

Here $\bar{S}_e = \frac{S_e}{S_\Delta}$; $\bar{C}_{Ae} = \frac{C_{Ae}}{l_{\Delta/2}}$ are the elevon area ratio and mean aerodynamic chord ratio up to the hinge line, respectively.

In the case of an elevon constant absolute chord the hinge-line coefficient will be equal

$$\bar{C}_{he} = -\frac{1}{57{,}3} \frac{4\operatorname{tg}\varepsilon \bar{C}_e^2}{\bar{S}_e C_{Ae} \beta} \left(\bar{b}_e - \frac{4\bar{C}_e}{3\pi\beta} \right) \quad (33)$$

The comparison of calculated and experimental characteristics of the hinge-moments showed that the design values of the hinge-moment were somewhat overestimated. Therefore, when estimating the elevon hinge-moments at moderate supersonic speeds the design value of the coefficient C_{he} which has been found from the formula (29) must be multiplied by the empirical coefficient $K \cong 0{,}85$.

III. An Investigation of a Physical Picture of Flow Past the Low-Aspect-Ratio Wing with Deflected Elevons by the Pressure Distribution Method

An investigation of a physical picture of flow past the wing with the elevon deflected was conducted on the model of the low-aspect-ratio wing with the variable-sweep leasing edge (fig.8). The analysis of the effect of free-stream Mach number on the flow about the wing with the elevon deflected has been illustrated by the example of considering the pressure diagram at the wing section approximately at the elevon midspan.

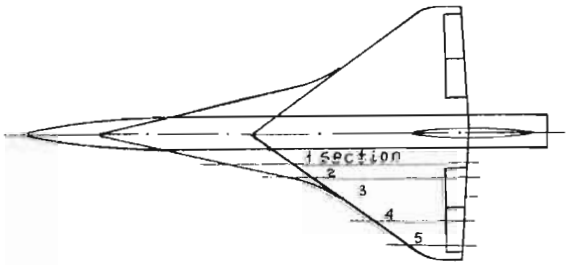

FIGURE 8

The diagram of the pressure distribution along the chord of the wing with the deflected elevon at M=0,6 is given in fig. 9.

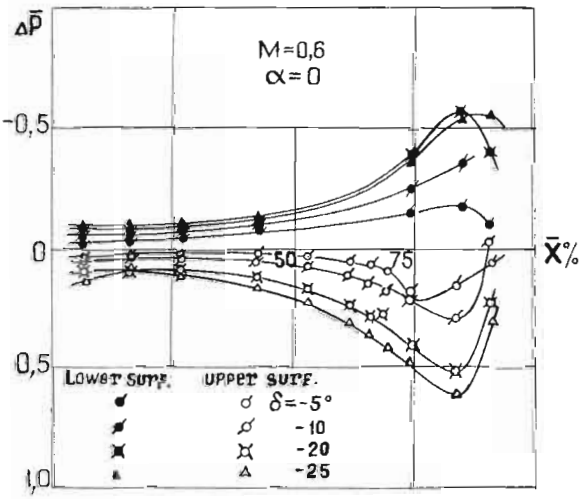

FIGURE 9

Here it is seen that the elevon deflection produces the change of the pressure distribution along the whole chord of the wing over both the upper and lower surfaces. At M=0,83 (fig. 10) the elevon negative deflection produces no longer the change of the pressure distribution along the whole chord over the wing lower surface.

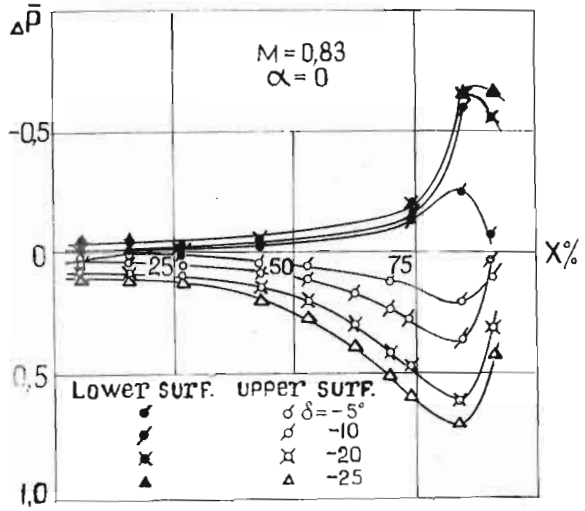

FIGURE 10

When passing to low supersonic speeds (M=1,05) the elevon negative deflection produces the change of the pressure distribution over the lower surface of the wing only along the elevon chord (fig.11), but over the upper wing surface the elevon deflection effect on the change of the pressure distribution spreads forward the further the more elevon deflection.

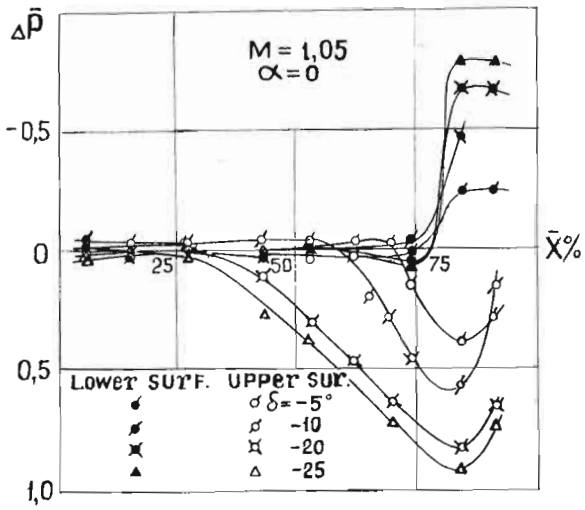

FIGURE 11

A similar situation occurs at high free-stream Mach numbers but the higher Mach number the less the elevon influence spreads forward from the elevon on the pressure surface (fig. 12).

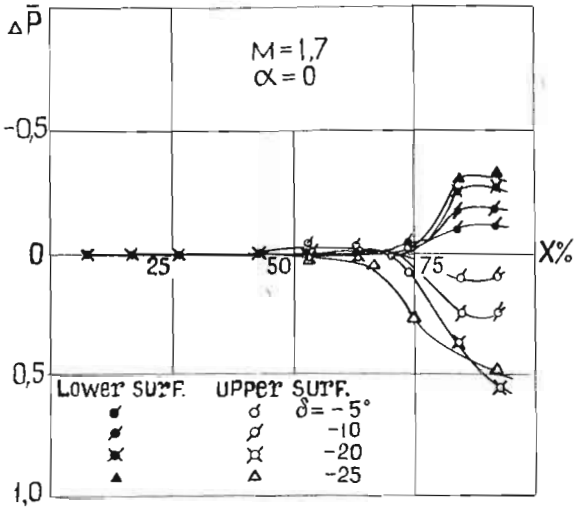

FIGURE 12

When passing from subsonic speeds to supersonic ones the pressure diagram changes its shape on the elevon itself. If at subsonic speeds the pressure diagram shape is similar to triangular one, at supersonic speeds the shape of the diagram of pressure distribution along the elevon chord is similar to rectangular one.

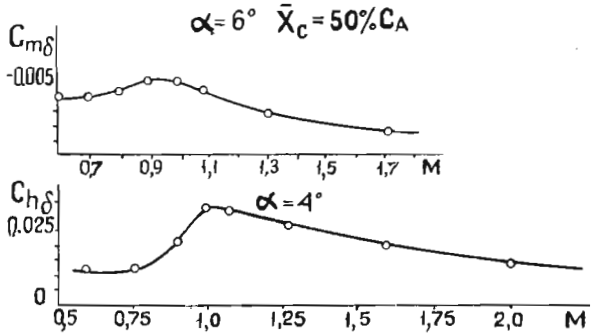

FIGURE 13

The aforementioned features of changes in behaviour of flow past the wing with deflected elevons account for reasons of elevon effectiveness loss and elevons hinge moments growth while passing from subsonic speeds to supersonic ones (fig. 13).

References

1. Belotserkovskii S.M. "Thin Lifting Surface in Subsonic Gas Flow". Publication "Nauka", 1965.

2. Mikeladze V.G. "An Investigation of Elevon Aerodynamic Characteristics on Low-Aspect-Ratio Wings". CAGI, Scientific Notes, vol. 1, N 2, 1970.